Analyst

Accepted Manuscript

ROYAL SOCIETY OF CHEMISTRY

www.rsc.org/analyst

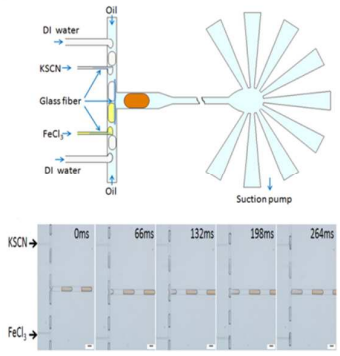

Serial additions of reagents with controlled volumes were performed using a glass fiber-induced droplet coalescence method without the requirement of external powers.

Cite this: DOI: 10.1039/c0xx00000x

www.rsc.org/xxxxxx

ARTICLE TYPE

Precise quantitative addition of multiple reagents into droplets in sequence using glass fiber-induced droplet coalescence

Chunyu Li, Jian Xu, Bo Ma*

Received (in XXX, XXX) Xth XXXXXXXXX 20XX, Accepted Xth XXXXXXXXX 20XX

DOI: 10.1039/b000000x

Precise quantitative addition of multiple reagents into droplets in sequence is still a bottleneck in droplet-based analysis. To address this issue, we presented a simple and robust glass fiber-induced droplet coalescence method. The hydrophilic glass fiber embedded in the microchannels can induce the deformation of droplets and trigger the coalescence. Serial additions of reagents with controlled volumes were performed by this method without the requirement of external powers.

In droplet-based microfluidic systems, each discrete droplet with volumes from femo to nanoliter can be used as an independent microreactor. Compare to microplate or tube based assays, droplet microfluidics has the promising advantages of performing high-throughput assays with minimal sample consumption, reduced reaction time, and low risk of cross contamination. It has shown great potentials in enzyme kinetics[1, 2], cell culture and screening[3, 4], and nucleic acid assays[5, 6]. For complex biological and chemical assays, multiple reagent addition is usually required. However, unlike the microtiter plates or test tubes, it is hard to add new reagents into the droplet, especially multiple reagent addition, once a stable water-oil interface of the droplet is formed. A simple, easy-to-use method enabling the addition of reagents into the droplet with controlled quantities and sequence without the requirement of external powers is still needed.

Existing methods for the addition of reagents into droplets can be categorized: droplet coalescence and direct injection. For the droplet coalescence, external energies such as electrical field[7-10], heat[11], and laser[12] were exploited to merge droplets. Besides, the passive methods[13, 14], such as special geometry structures[15-18] or the surface energy of the walls of microchannels[19], also can induce the droplet coalescence, which eliminates the requirement of external energy sources. However, addition of reagents in a controllable sequence is not easy to be dealt with using these methods due to the difficulty of droplet synchronization. For direct injection, the reagent injected by side channels as a continuous phase is directly added into existing droplets[20-23]. But, injecting of reagents into droplets is limited to volumetric injection ratio.

We presented a simple and robust glass fiber-induced droplet coalescence method for reliable multiple reagent addition. The hydrophilic glass fibers embedded in the microchannels induce the coalescence of the surfactant-stabilized droplet pairs. This method has some advantages over existing methods. By exploiting this method, multiple reagents were added into droplets with precisely controlled addition volume sequentially. Volumetric addition ratio can be tuned in a flexible way. Moreover, based on our previous work[24], this passive droplet coalescence method was performed on a self-powered microfluidic droplet platform in which air-evacuated PDMS was used as an internal power source for droplet generation and manipulation. Good compatibility with the self-powered microfluidic droplet platform makes this method have a great potential in in-field droplet-based analysis.

In this work, the microfluidic chip was fabricated in PDMS by soft lithography technology[25]. Briefly, a SU-8 mold was firstly fabricated using standard photolithography technology. The PDMS precursor and curing agent (Sylgard 184, Dow Corning, USA) were thoroughly mixed in a weight ratio of 10:1 and degassed in vacuum. The curing mixture was poured onto the SU-8 mold and cured in an oven for 2 h at 80℃. To induce the droplet coalescence, glass fibers (diameter in 5-30μm), which were pulled from the glass rod with diameter in 1mm by the glass puller (PN-31, Narishige, Japan), were embedded in the pre-fabricated PDMS slab embossed with microfluidic channels under the light microscope. This process usually only took about 1-2 minutes. Then, the PDMS slab embedded the glass fiber was irreversibly bonded with another piece of flat PDMS slab under oxygen plasma treatment. The sealed PDMS chip was placed in the oven for at least 12h at 80℃ to recover its hydrophobicity. An alternative simple fabrication method was to directly bond two pieces of PDMS slabs without oxygen plasma treatment due to negative pressure suction preventing fluid leakage. The height of all the channels/chambers was ~60μm.

Before use, the PDMS chip was degassed for 10min in a vacuum desiccator. Then, the aqueous solution and mineral oil (viscosity: 34cP at 20℃ and density: 0.84g/cm^3) containing 2.5% (v/v) Span 80 were pipetted into the inlets rapidly. The process of droplet generation and coalescence was recorded with an inverted microscope (IX71, Olympus, Japan) equipped with a charge-coupled device (CCD) camera (DP72, Olympus, Japan). The collected images were processed and analyzed using Image Pro Plus 6.0 software.

As shown in Fig.1a, the microfluidic chip consisted of three T-junctions and a suction pump. The suction pump is designed as the dead-ended chambers arranged in a fan shape, which utilizes the air-evacuated PDMS to produce a persistent internal driving

force[26, 27]. Two T-junctions located at the two wings are used for the generation of droplets. The middle one embedded with the glass fiber is used for the droplet coalescence. Christopher et.al investigated the collision behaviors of droplets at the junctions where droplet pairs have the similar size and move in opposite direction[17]. They observed the droplet coalescence probably occurred at a low collision speed. But this phenomenon may be attributed to no surfactant addition. In our experiments, we found the coalescence of the surfactant-stabilized droplets is hard to be achieved by colliding at the microfluidic junction (Fig.1c and Movie 1). Next, the glass fibers with different surface properties were placed into the junction. The hydrophobic surface of the glass fiber was fabricated by coating the ultra-thin PDMS film onto the glass fibers. As shown in Fig.1c, the droplet coalescence was triggered by the hydrophillic glass fiber (Movie 3) but not the hydrophobic glass fiber (Movie 2). Thus, we deduced that the hydrophilic surface of the glass fiber could be a key factor to induce the droplet coalescence. Localized surface energy change of the microchannel caused by the embedded glass fiber could induce the instability of droplet edges and trigger the coalescence. To further verify this, we tried other hydrophilic fibers such as the cotton fiber. As expected, the droplet coalescence was easily achieved (see Fig.S1 in the supplementary information).

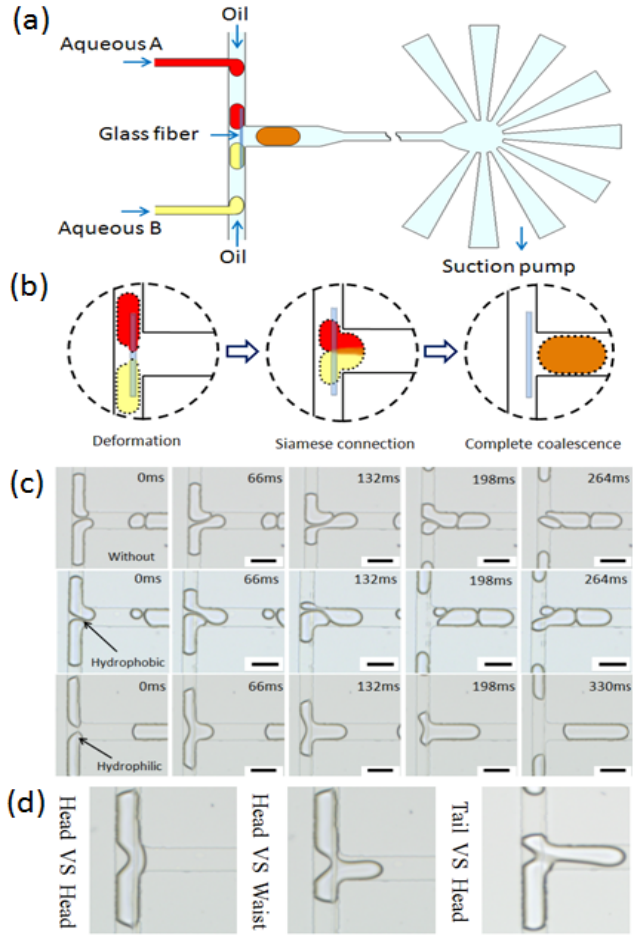

Fig.1 Coalescence of two similar-sized droplets. (a) Schematic diagram of the chip. (b) Process of the glass fiber induced coalescence. (c) Collision behaviors of two droplets at the junction with and without embedded glass fibers. The diameter of the glass fiber was ~10μm. (d) Siamese connections of two droplets with different shapes due to timing difference between the arrivals of droplets at the junction. The droplet was divided into three equal parts which were labeled as head, waist, and tail along the direction of flow, respectively. Aqueous A and B both were DI water. Sample volumes both were 4μL. Scale bar represented 100μm.

According to observations, we divided the process of the glass fiber induced droplet coalescence into three subsequent phases: deformation, siamese connection, and complete coalescence (Fig.1b and 1c). When droplets flowed past the glass fiber, the spreading of droplets on the hydrophilic glass fiber induced the localized deformation of droplet edges, resulting in the instability of the water-oil interface. Once deformed edges of two droplets were in contact with each other on the glass fiber, the coalescence was triggered and the siamese connection was formed. And then the coalescence of two droplets extended from initial point to entire body of the droplet pair. Finally, two droplets were merged to a single droplet.

Synchronization of droplet pairs is an essential prerequisite for the droplet coalescence. In this scenario, symmetric design of two droplet generation components (T-junctions) and the same drawing force provided by the suction pump were adopted, which facilitate the synchronized production of droplet pairs. Moreover, the glass fiber induced coalescence can be triggered in any part of two colliding droplets (Fig.1d), which further compensates tiny timing difference between the arrivals of the droplet pair at the junction. Thus, these strategies and characteristic of the coalescence ensure reproducible and reliable droplet coalescence (at least 20 experiments in different chips).

We further investigated effects of the glass fiber diameter and length on the droplet coalescence. We observed that the glass fibers with different diameters (5μm, 10μm, 20μm, and 30μm) all induced the droplet coalescence. But as the diameter of the glass fiber increased to 30μm, the droplet completely spread on the glass fiber (see Fig.S2 in the supplementary information). The merging droplet pair did not form the confined siamese connection structure and they detached from the glass fiber just like the process of droplet formation. This could be attributed to increased hydrophilic surface areas. We also found the length of the glass fibers did not significantly influence the efficiency of the coalescence (data not shown). But considering the stability of the embedded glass fibers, the length of the glass fibers should be larger than the width of the T-junction convergence.

We can perform reagent addition with approximate 1:1 stoichiometry by the coalescence of two similar-sized droplets at the junction. However, it is difficult to merge two droplets with dramatically different sizes using this design since the velocity difference between droplets leads to the difficulty of synchronization. To realizing small-volume addition by a small droplet merging with a large one, we designed a double T-shaped channel in which two T-junctions are used to generated large and small droplets respectively (Fig.2a). Glass fibers are embedded into the downstream junction to trigger the droplet coalescence. The expanded region in the main channel is used to accelerate mixing of droplet contents and does not involve in the droplet coalescence. In this scenario, the flow rate of the oil phase was fixed. To generate droplets with different sizes, the flow rate of the aqueous phase was tuned by the flow resistance of aqueous phase channels (width of the upstream aqueous phase channel: 25μm; width of the downstream aqueous phase channel: 10μm).

We labeled the large droplet generated from upstream T-junction as the 'receive' droplet and the small one generated from downstream T-junction as the 'feed' droplet. In addition, to fasten the glass fiber into the channel, the selected diameter (15μm) of the glass fiber was larger than width of the downstream aqueous phase channel.

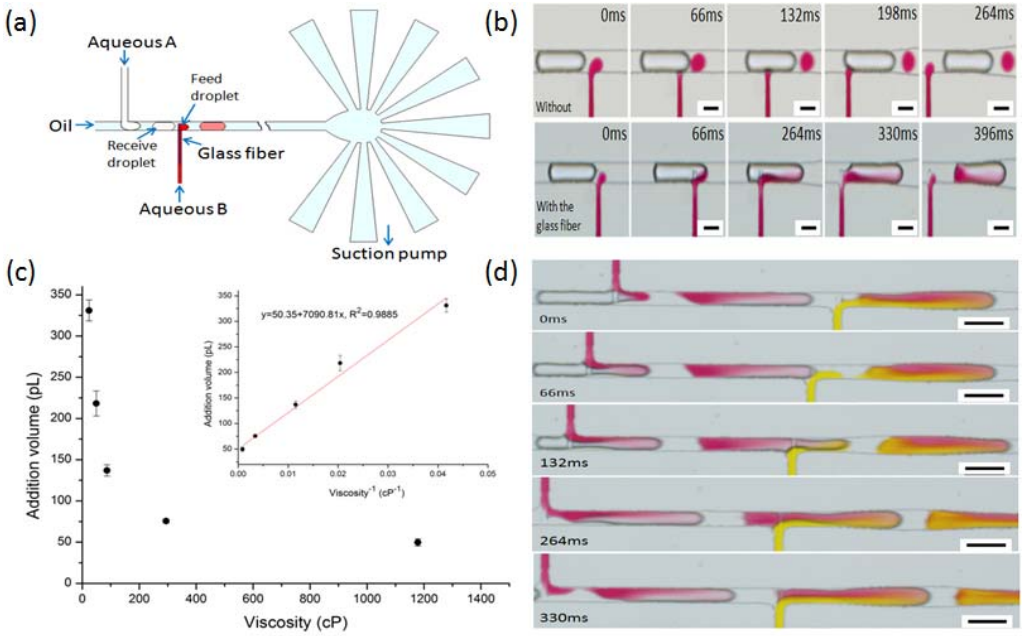

Fig.2 Coalescence of droplets with different sizes. (a) Schematic diagram of the chip. (b) Collision behaviors of droplets with different sizes at the junction with and without embedded glass fibers. Scale bar represented 50μm. (c) Effect of the viscosity of the downstream aqueous phase on addition volume. Error bar represents standard deviation. (d) Sequential additions of different reagents into the receive droplet. Scale bar represented 100μm. In all experiments, the upstream aqueous phase was DI water and sample volume was 4μL. Sample volume of downstream aqueous phase containing dyes was 1μL. In the (b) and (d), downstream aqueous phase contained 83% glycerol.

As shown in Fig.2b and Movie 4, no coalescence events occurred when the receive droplet and the 'feed' droplet came into contact with each other in the chip without the glass fiber. In the chip embedded with the glass fibers, the newborn 'feed' droplet stuck to the glass fiber due to its hydrophilic surface and grew until the incoming 'receive' droplet touched and merged with it (Movie 5). Hydrophilic glass fiber that induces instability of the water-oil interface could play a dominant role in the droplet coalescence. We observed that the coalescence occurred during two droplets detached from the glass fiber instead of impacting each other. This phenomenon could be explained by the fact that decompressing droplets facilitate the coalescence[28]. In this design, there are two key points to ensure the droplet coalescence. Firstly, the hydrophilic glass fiber should penetrate into the main channel. Secondly, the frequency should be matched between the 'receive' droplet passing the downstream junction and the 'feed' droplet forming. When these requirements are met, the efficiency of the droplet coalescence is 100% (> 20 experiments in different chips).

Hydrophilic surface of the glass fiber could bring a potential risk of contamination between droplets. This is a common issue for hydrophilic surface induced droplet coalescence method. One way to solve this problem is to reduce contact areas between droplets and the hydrophilic surface. Compare to reported methods[29], this method has much smaller contact area. Real contact area between droplets and the glass fibers was only ~1.2×10^{-3}mm^2 (diameter of the glass fiber: ~15μm, length of penetrating into the main channel: ~25μm). Moreover, surface modification of the glass fiber could be considered to further reduce the non-specific adsorption

Next, we investigated the feasibility of precisely controlling addition volume. The size of the 'feed' droplet that is related to the flow rate of the downstream aqueous phase mainly determines the addition volume. Unlike the syringe pump driven system, the absolute flow rate in the air-evacuated PDMS chip is not easy to be evaluated accurately. However, according to hagen-poiseuille's law, the flow rate is relevant to pressure, flow resistance, and viscosity of liquid. So, the droplet size can be precisely tuned by these factors. In our previous work, we have demonstrated that the droplet size can be adjusted by the flow resistance of the channel or the hydrostatic pressure exerted on the aqueous phase in the degassed-PDMS based droplet generator[24]. Here, we adopted an alternative method that tuned the droplet size by the viscosity of the downstream aqueous phase. We changed the concentration of glycerol in water to prepare the aqueous solution with different viscosity (see Table S1 in the supplementary information). Addition volumes were calculated by measuring the change in droplet size before and after the coalescence. As shown in Fig.2c, Fig.S3 and Movie 6-10, addition volumes reduced with the increase of the viscosity of the downstream aqueous phase. The Hagen-Poiseuille equation shows that the flow rate is proportional to the reciprocal of viscosity of liquid. According to this, addition volumes were plotted against the reciprocal of the viscosity of the downstream aqueous phase. A linear relationship between them was obtained. Small volumes of reagents (50-331pL) can be added into the 'receive' droplet (580pL before coalescence). The exact amount of reagents can be precisely controlled by adjusting the flow rate.

In this method, a side channel embedded with the glass fiber can be used as a pipettor. This pipettor, which only occupies tens micron space along the main channel, could be compactly integrated into the microchip. The serial piptettors along the channel enable the sequential addition of reagents. The drag force produced by the suction pump provides a driving force for the generation of 'receive' and 'feed' droplets. To demonstrate it, we fabricated a chip with two piptettors in series along the channel. As shown in Fig.2d and Movie 11, red and yellow dyes represented different reagents were added into the receive droplet in sequence. This result showed the ability of this method to control the order of the addition of reagents.

As mentioned above, two strategies for the droplet coalescence have been investigated. These strategies which both rely on the glass fiber induced coalescence are complementary. One is suitable for two similar-sized droplets, another one is suitable for two different size droplets. Merging two strategies into a single chip could allow a flexible volumetric addition ratio between the reagent volumes and the droplet volumes. As shown in Fig.3a, two blank droplets containing DI water received the droplets of $FeCl_3$ and KSCN, respectively, and then were merged into a single droplet. The coalescence triggered the chemical reaction within milliseconds. The colored $Fe(SCN)^{2+}$ complex produced in the droplet (Fig.3b and Movie 12). Multiple reagent addition with controlled addition sequence and volumes was performed, which indicates this passive droplet coalescence method has the potential to accomplish more complex biological and chemical analysis.

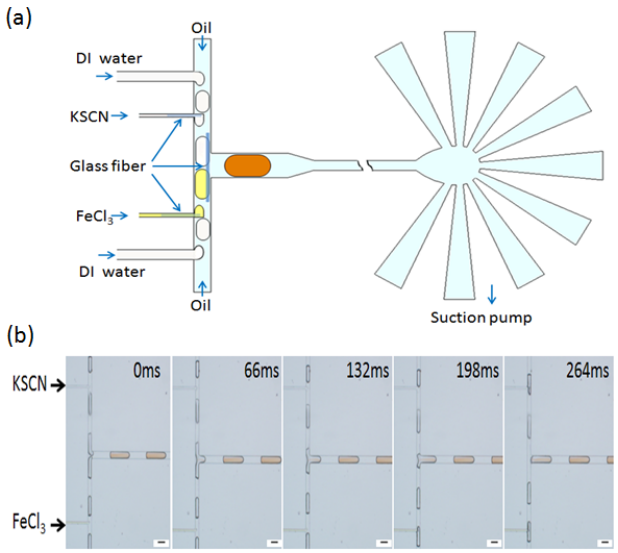

Fig.3 Multiple reagent addition. (a) Schematic diagram of the chip. (b) Two blank droplets coming from two sides merged with the droplets of $FeCl_3$ and KSCN, respectively. At the middle junction, they merged into a single droplet in which $FeCl_3$ reacted with KSCN and produced colored $Fe(SCN)^{2+}$. Sample volumes of $FeCl_3$ and KSCN solution containing 83% glycerol both were 1μL. Sample volumes of DI water both were 4μL.

Conclusions

In summary, we have demonstrated a simple and robust glass fiber-induced method for the droplet coalescence. Reliable multiple additions with the precise control of addition volume and sequence were achieved. Moreover, we demonstrated this passive method can match with an air-evacuated PDMS microfluidic platform in which the generation and coalescence of droplets can be smoothly accomplished without the requirement of external powers. This work will take a first and important step to set up an integrated, self-contained droplet-based analytical system for the point of care analysis.

Acknowledgment

This work was supported by Basic Research in Scientific Instrument Program and general program from National Natural Science Foundation of China (No. 31327001, 31470220), Scientific Instrument Development Program from the Chinese Academy of Sciences (No. YZ201236), Key Deployment Grant on Modern Agriculture from the Chinese Academy of Sciences (No. KSZD-EW-Z-021-1-5).

Notes and references

Single-Cell Center, CAS Key Laboratory of Biofuels and Shandong Key Laboratory of Energy Genetics, Qingdao Institute of Bioenergy and Bioprocess Technology, Chinese Academy of Sciences, Qingdao, Shandong 266101, China

**Corresponding author: Bo Ma; E-mail: mabo@qibebt.ac.cn; Tel: +86 -532-80662657; Fax: +86 -532-80662654*

†Electronic Supplementary Information (ESI) available: [Supplementary information, Movie 1-12].

1. H. Song and R. F. Ismagilov, *Journal of the American Chemical Society*, 2003, **125**, 14613-14619.
2. M.-P. N. Bui, C. A. Li, K. N. Han, J. Choo, E. K. Lee and G. H. Seong, *Analytical Chemistry*, 2011, **83**, 1603-1608.
3. J. Clausell-Tormos, D. Lieber, J. C. Baret, A. El-Harrak, O. J. Miller, L. Frenz, J. Blouwolff, K. J. Humphry, S. Koster, H. Duan, C. Holtze, D. A. Weitz, A. D. Griffiths and C. A. Merten, *Chem. Biol.*, 2008, **15**, 427-437.
4. E. Brouzes, M. Medkova, N. Savenelli, D. Marran, M. Twardowski, J. B. Hutchison, J. M. Rothberg, D. R. Link, N. Perrimon and M. L. Samuels, *Proceedings of the National Academy of Sciences of the United States of America*, 2009, **106**, 14195-14200.
5. N. R. Beer, E. K. Wheeler, L. Lee-Houghton, N. Watkins, S. Nasarabadi, N. Hebert, P. Leung, D. W. Arnold, C. G. Bailey and B. W. Colston, *Analytical Chemistry*, 2008, **80**, 1854-1858.
6. Y. Zeng, R. Novak, J. Shuga, M. T. Smith and R. A. Mathies, *Analytical Chemistry*, 2010, **82**, 3183-3190.
7. M. Zagnoni and J. M. Cooper, *Lab on a Chip*, 2009, **9**, 2652-2658.
8. M. Chabert, K. D. Dorfman and J. L. Viovy, *Electrophoresis*, 2005, **26**, 3706-3715.
9. M. Zagnoni, C. N. Baroud and J. M. Cooper, *Physical Review E*, 2009, **80**.
10. M. Zagnoni, G. Le Lain and J. M. Cooper, *Langmuir*, 2010, **26**, 14443-14449.
11. B. Xu, N. Nam-Trung and T. N. Wong, *Biomicrofluidics*, 2012, **6**.
12. Z. G. Li, K. Ando, J. Q. Yu, A. Q. Liu, J. B. Zhang and C. D. Ohl, *Lab on a Chip*, 2011, **11**, 1879-1885.
13. L. Mazutis, J.-C. Baret and A. D. Griffiths, *Lab on a Chip*, 2009, **9**, 2665-2672.
14. L. Mazutis and A. D. Griffiths, *Lab on a Chip*, 2012, **12**, 1800-1806.
15. X. Niu, S. Gulati, J. B. Edel and A. J. deMello, *Lab on a Chip*, 2008, **8**, 1837-1841.
16. L. H. Hung, K. M. Choi, W. Y. Tseng, Y. C. Tan, K. J. Shea and A. P. Lee, *Lab on a Chip*, 2006, **6**, 174-178.
17. G. F. Christopher, J. Bergstein, N. B. End, M. Poon, C. Nguyen and S. L. Anna, *Lab on a Chip*, 2009, **9**, 1102-1109.
18. Y.-C. Tan, Y. L. Ho and A. P. Lee, *Microfluidics and Nanofluidics*, 2007, **3**, 495-499.
19. L. M. Fidalgo, C. Abell and W. T. S. Huck, *Lab on a Chip*, 2007, **7**, 984-986.

20. A. R. Abate, T. Hung, P. Mary, J. J. Agresti and D. A. Weitz, *Proceedings of the National Academy of Sciences of the United States of America*, 2010, **107**, 19163-19166.
21. H. Song, H.-W. Li, M. S. Munson, T. G. Van Ha and R. F. Ismagilov, *Analytical Chemistry*, 2006, **78**, 4839-4849.
22. L. Li, J. Q. Boedicker and R. F. Ismagilov, *Analytical Chemistry*, 2007, **79**, 2756-2761.
23. A. M. Nightingale, T. W. Phillips, J. H. Bannock and J. C. de Mello, *Nature Communications*, 2014, **5**.
24. C.Y.Li, J.Xu,B.Ma, *Microfluidics and Nanofluidics*, 2014, **DOI: 10.1007/s10404-014-1497-5**.
25. D. C. Duffy, J. C. McDonald, O. J. A. Schueller and G. M. Whitesides, *Analytical Chemistry*, 1998, **70**, 4974-4984.
26. K. Hosokawa, K. Sato, N. Ichikawa and M. Maeda, *Lab on a Chip*, 2004, **4**, 181-185.
27. K. Hosokawa, M. Omata, K. Sato and M. Maeda, *Lab on a Chip*, 2006, **6**, 236-241.
28. N. Bremond, A. R. Thiam and J. Bibette, *Physical Review Letters*, 2008, **100**.
29. Y. Liu and R. F. Ismagilov, *Langmuir*, 2009, **25**, 2854-2859.